

Calibration of the LIBOR market model - implementation in PREMIA*

Nicolas PRIVAULT

Department of Mathematics
City University of Hong Kong
Tat Chee Avenue
Kowloon Tong, Hong Kong

Xiao WEI

School of Insurance
Central University of Finance and Economics
100081, Beijing, P.R. China

Abstract

This paper reviews the BGM model for the parameterization of LIBOR forward interest rate curves, and presents a C++ implementation in PREMIA of the calibration algorithm of [7] using the market prices of caps and swaptions in this model.

Keywords: LIBOR market model, BGM model, interest rates, caps, swaps, calibration.

1 Introduction

The calibration of the Brace-Gatarek-Musiela (BGM) and Jamshidian LIBOR interest rate model to the market values of caps and swaptions has proved to involve several numerical stability issues.

*This work was carried out while both authors were at INRIA Rocquencourt, Projet MathFi, BP 105, 78153 Le Chesnay Cedex, France.

In this paper we describe a C++ implementation in PREMIA of the stable algorithm for the joint calibration of [7] for the LIBOR market model, from the prices of caps and swaptions.

The outline of this paper is as follows. In Section 2 we recall the definition of forward rates and contracts, and in Section 3 we present the arbitrage free modeling of zero coupon bonds, cf. [2], [5], [3] for details. In Section 4 we re-derive the BGM model using Itô calculus, cf. [1], [4]. The pricing of caps and swaptions in this model is described in Section 5. Section 6 is devoted to the calibration algorithm of [7].

2 Zero coupon bonds and forward rates

Consider a short term interest rate process $(r_t)_{t \in \mathbb{R}_+}$ given by

$$dr_t = \mu_t(r_t)dt + \sigma_t^\dagger(r_t) \cdot dB_t, \quad t \in \mathbb{R}_+,$$

where $(B_t)_{t \in \mathbb{R}_+}$ is a standard Brownian motion in \mathbb{R}^d . A zero-coupon bond based on $(r_t)_{t \in \mathbb{R}_+}$ is a contract made at time $t < T$ to deliver $P(T, T) = 1\$$ at time T , and valued

$$P(t, T) := \mathbb{E} \left[\exp \left(- \int_t^T r_s ds \right) \middle| r_t \right].$$

Figure 2.1 presents a random simulation of $t \mapsto P(t, T)$ in the Vašiček model, combined with the graph of the corresponding deterministic interest rate compounding.

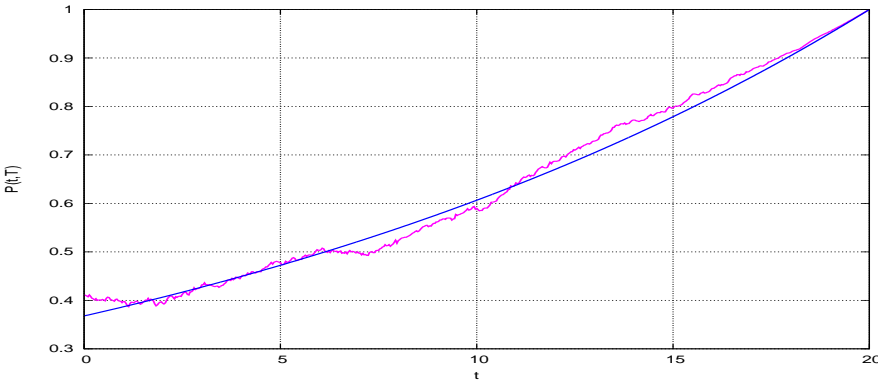


Figure 2.1: $t \mapsto P(t, T)$ and $t \mapsto e^{-r_0(T-t)}$.

The instantaneous forward rate process, given by

$$T \mapsto f(t, T) = -\frac{\partial \log P(t, T)}{\partial T},$$

is represented in Figure 2.2 in the Vašiček model used in Figure 2.1:

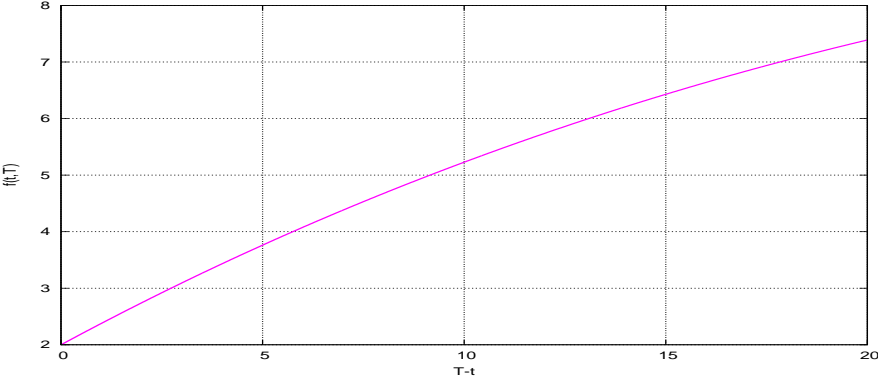


Figure 2.2: Instantaneous forward rate process $T \mapsto f(t, T)$.

The (simply compounded) forward rate is defined as:

$$F(t, T, S) := \frac{1}{S - T} \left(\frac{P(t, T)}{P(t, S)} - 1 \right), \quad 0 \leq t \leq T < S,$$

i.e. the interest rate contracted at time t for a loan over the future period $[T, S]$:

$$P(t, T) - P(t, S) = P(t, S)(S - T)F(t, T, S), \quad 0 \leq t \leq T < S.$$

The forward rate agreement at time t gives its holder the right to an interest rate $F(t, T, S)$ on the time period $[T, S]$. Next (Figure 2.3) is a simulation of the simply compounded spot rates $L(t, T)$ defined as $L(t, T) = F(t, t, T)$, and computed from the sample graphs of Figure 2.1:

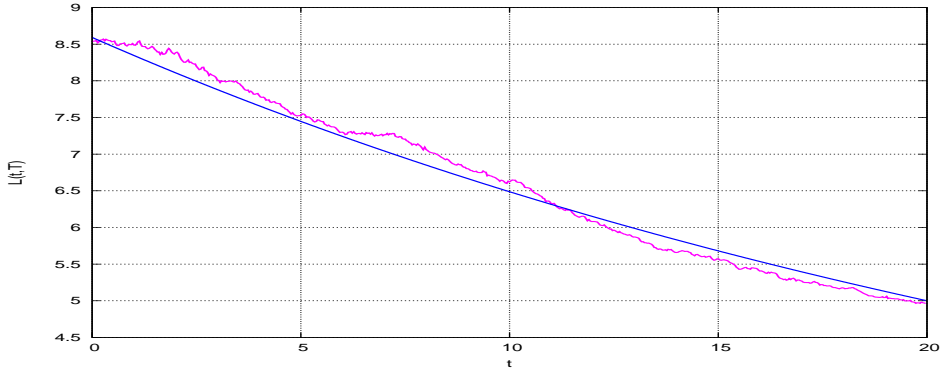


Figure 2.3: $t \mapsto L(t, T) = F(t, t, T)$.

The forward curve $T \mapsto F(0, T, T + \delta)$ is plotted in Figure 2.4 for $t = 0$ in the Vašiček model used in Figure 2.1:

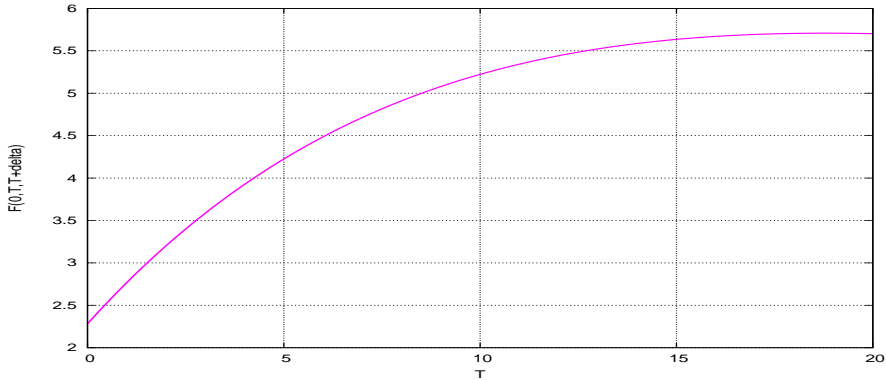


Figure 2.4: $T \mapsto F(0, T, T + \delta)$.

In practice, the maturity dates are arranged according to a discrete tenor structure

$$0 = T_0 < T_1 < T_2 < \dots < T_n,$$

with $\delta_i = T_{i+1} - T_i$, $i = 1, \dots, n-1$. An example of data used for the forward interest rate curve is given in Figure 2.5, with here $t = 07/05/2003$ and $\delta = \text{one year}$:

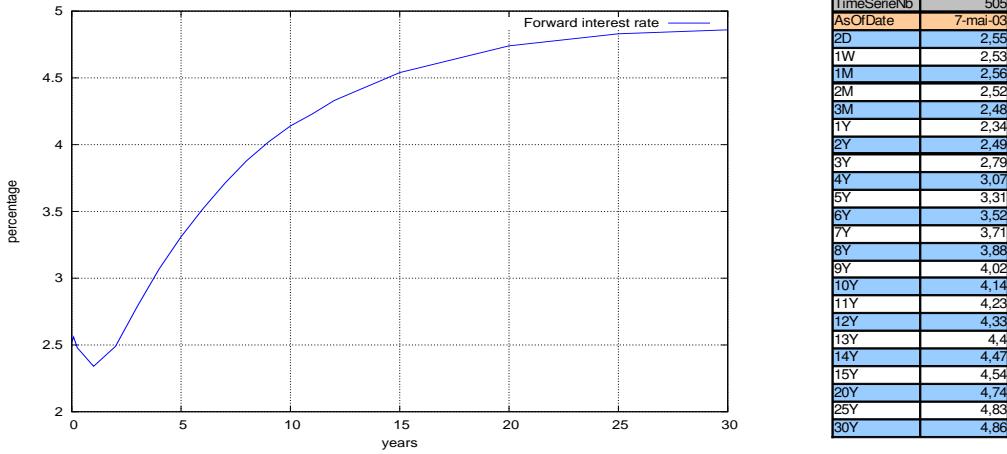


Figure 2.5: $T \mapsto F(t, T, T + \delta)$.

Note that actual data of forward interest rate curves can also be fitted by parametric methods as in e.g. the Nelson-Siegel model. More generally, the forward swap rate process

$$S(t, T_i, T_j) = \frac{P(t, T_i) - P(t, T_j)}{P(t, T_i, T_j)}, \quad t \in [0, T_i], \quad 1 \leq i < j \leq n,$$

is defined from

$$0 = P(t, T_j) - P(t, T_i) + S(t, T_i, T_j) \sum_{k=i}^{j-1} \delta_k P(t, T_{k+1}), \quad t \in [0, T_i], \quad 1 \leq i < j \leq n,$$

where

$$P(t, T_i, T_j) = \sum_{k=i}^{j-1} \delta_k P(t, T_{k+1}), \quad t \in [0, T_i], \quad 1 \leq i < j \leq n,$$

is the annuity numeraire, with the relation

$$P(t, T_j) = \frac{P(t, T_i) - S(t, T_i, T_j) \sum_{k=i}^{j-2} \delta_k P(t, T_{k+1})}{1 + \delta_{j-1} S(t, T_i, T_j)}, \quad t \in [0, T_i], \quad 1 \leq i < j \leq n.$$

When $j = i+1$, the swap rate $S(t, T_i, T_{i+1})$ coincides with the forward rate $F(t, T_i, T_{i+1})$, and we recover the discount factor $P(t, T_i)$ from $S(t, T_i, T_{i+1}) = F(t, T_i, T_{i+1})$ using the relations

$$P(t, T_{i+1}) = \frac{P(t, T_i)}{1 + \delta_i S(t, T_i, T_{i+1})}, \quad t \in [0, T_i], \quad 0 \leq i \leq n-1.$$

3 Arbitrage free modeling

From now on we assume that the dynamics of $P(t, T_i)$ under the risk neutral probability measure is given by

$$\frac{dP(t, T_i)}{P(t, T_i)} = r_t dt + \zeta_i^\dagger(t) \cdot dW_t, \quad i = 1, \dots, n,$$

where $(r_t)_{t \in \mathbb{R}_+}$ and $(\zeta_i(t))_{t \in \mathbb{R}_+}$, $i = 1, \dots, n$, are adapted with respect to the filtration $(\mathcal{F}_t)_{t \in \mathbb{R}_+}$ generated by the \mathbb{R}^d -valued Brownian motion $(W_t)_{t \in \mathbb{R}_+}$, under the assumption (absence of arbitrage condition) that

$$t \mapsto e^{-\int_0^t r_s ds} P(t, T_i), \quad t \in [0, T_i], \quad i = 1, \dots, n,$$

is an \mathcal{F}_t -martingale under \mathbb{P} .

Definition 3.1. Let the probability measure \mathbb{P}_i be defined as

$$\frac{d\mathbb{P}_i}{d\mathbb{P}} = \frac{1}{P(0, T_i)} e^{-\int_0^{T_i} r_s ds}, \quad i = 1, \dots, n.$$

Note that for $i = 1, \dots, n$, we have

$$\mathbb{E} \left[\frac{d\mathbb{P}_i}{d\mathbb{P}} \middle| \mathcal{F}_t \right] = \frac{1}{P(0, T_i)} \mathbb{E} \left[e^{-\int_0^{T_i} r_s ds} \middle| \mathcal{F}_t \right] = \frac{P(t, T_i)}{P(0, T_i)} e^{-\int_0^t r_s ds}, \quad t \in [0, T_i].$$

Moreover, for all $i = 1, \dots, n$ we have

$$\frac{d\mathbb{P}_{i|\mathcal{F}_t}}{d\mathbb{P}_{|\mathcal{F}_t}} = \frac{e^{-\int_t^{T_i} r_s ds}}{P(t, T_i)}, \quad t \in [0, T_i]. \quad (3.1)$$

Indeed, for all bounded and \mathcal{F}_t -measurable random variables G ,

$$\begin{aligned} \mathbb{E} \left[G F e^{-\int_t^{T_i} r_s ds} \right] &= P(0, T_i) \mathbb{E}_i \left[G e^{\int_0^t r_s ds} F \right] \\ &= P(0, T_i) \mathbb{E}_i \left[G e^{\int_0^t r_s ds} \mathbb{E}_i[F \mid \mathcal{F}_t] \right] \\ &= \mathbb{E} \left[G e^{-\int_t^{T_i} r_s ds} \mathbb{E}_i[F \mid \mathcal{F}_t] \right] \\ &= P(t, T_i) \mathbb{E} [G \mathbb{E}_i[F \mid \mathcal{F}_t]], \end{aligned}$$

hence

$$\mathbb{E} \left[F e^{-\int_t^{T_i} r_s ds} \middle| \mathcal{F}_t \right] = P(t, T_i) \mathbb{E}_i[F \mid \mathcal{F}_t], \quad t \in [0, T_i],$$

for all integrable random variables F . The next proposition will be useful to determine the dynamics of interest rate processes under \mathbb{P}_i .

Proposition 3.2. For $i = 1, \dots, n$, let

$$W_t^i := W_t - \int_0^t \zeta_i(s) ds, \quad 0 \leq t \leq T_i, \quad (3.2)$$

then $(W_t^i)_{t \in [0, T_i]}$ is a standard \mathbb{R}^d -valued Brownian motion under \mathbb{P}_i .

Proof. Letting

$$\Phi_i(t) = \mathbb{E} \left[\frac{d\mathbb{P}_i}{d\mathbb{P}} \middle| \mathcal{F}_t \right] = \frac{P(t, T_i)}{P(0, T_i)} e^{-\int_0^t r_s ds}, \quad t \in [0, T_i],$$

we have $d\Phi_i(t) = \Phi_i(t) \zeta_i^\dagger(t) \cdot dW_t$, hence by the Girsanov theorem,

$$W_t - \int_0^t \frac{1}{\Phi_i(s)} d\langle \Phi_i(s), W_s \rangle = W_t - \int_0^t \zeta_i(s) ds, \quad t \in [0, T_i],$$

is a continuous martingale under \mathbb{P}_i . \square

In the sequel, the expectation under \mathbb{P}_i will be denoted by \mathbb{E}_i .

Proposition 3.3. For all $1 \leq i, j \leq n$ we have

$$\mathbb{E}_i \left[\frac{d\mathbb{P}_j}{d\mathbb{P}_i} \middle| \mathcal{F}_t \right] = \frac{P(0, T_i)}{P(t, T_i)} \frac{P(t, T_j)}{P(0, T_j)}, \quad 0 \leq t \leq T_i \wedge T_j, \quad (3.3)$$

and in particular the process

$$t \mapsto \frac{P(t, T_j)}{P(t, T_i)}, \quad 0 \leq t \leq T_i \wedge T_j,$$

is an \mathcal{F}_t -martingale under \mathbb{P}_i , $1 \leq i, j \leq n$.

Proof. For all bounded and \mathcal{F}_t -measurable random variables F we have

$$\begin{aligned} \mathbb{E}_i \left[F \frac{d\mathbb{P}_j}{d\mathbb{P}_i} \right] &= \mathbb{E} \left[F \frac{d\mathbb{P}_j}{d\mathbb{P}} \right] \\ &= \frac{1}{P(0, T_j)} \mathbb{E} \left[F e^{-\int_0^{T_j} r_\tau d\tau} \right] \\ &= \frac{1}{P(0, T_j)} \mathbb{E} \left[F e^{-\int_0^t r_\tau d\tau} P(t, T_j) \right] \\ &= \frac{1}{P(0, T_j)} \mathbb{E} \left[F e^{-\int_0^{T_i} r_\tau d\tau} \frac{P(t, T_j)}{P(t, T_i)} \right] \\ &= \frac{P(0, T_i)}{P(0, T_j)} \mathbb{E}_i \left[F \frac{P(t, T_j)}{P(t, T_i)} \right], \end{aligned}$$

which shows (3.3). \square

By Itô's calculus we have, for any $i, j = 1, \dots, n$,

$$d \left(\frac{P(t, T_j)}{P(t, T_i)} \right) = \frac{P(t, T_j)}{P(t, T_i)} (\zeta_j(t) - \zeta_i(t))^\dagger \cdot (dW_t - \zeta_i(t) dt),$$

which, from Proposition 3.2, recovers the second part of Proposition 3.3, i.e. the martingale property of $P(t, T_j)/P(t, T_i)$. Note that if $1 \leq i < j \leq n$ we have

$$\frac{P(t, T_j)}{P(t, T_i)} = \prod_{k=i}^{j-1} \frac{1}{1 + \delta_k F(t, T_k, T_{k+1})}, \quad t \in [0, T_i],$$

and if $1 \leq j \leq i \leq n$,

$$\frac{P(t, T_j)}{P(t, T_i)} = \prod_{k=j}^{i-1} (1 + \delta_k F(t, T_k, T_{k+1})), \quad t \in [0, T_j].$$

4 Derivation of the BGM model

The aim of this section is to describe the Brace-Gatarek-Musiela (BGM) model, and in particular the BGM system of stochastic differential equations

$$\frac{dF(t, T_i, T_{i+1})}{F(t, T_i, T_{i+1})} = - \sum_{j=i+1}^{n-1} \frac{\delta_j F(t, T_j, T_{j+1})}{1 + \delta_j F(t, T_j, T_{j+1})} \gamma_i^\dagger(t) \cdot \gamma_j(t) dt + \gamma_i^\dagger(t) \cdot dW_t^n, \quad (4.1)$$

$0 \leq t \leq T_i$, where $\gamma_i(t)$ is a deterministic \mathbb{R}^d -valued function, $(W_t^n)_{t \in \mathbb{R}_+}$ is a standard Brownian motion in \mathbb{R}^d , and $F(t, T_i, T_{i+1})$, $0 \leq t \leq T_i$, is a martingale under \mathbb{P}_{i+1} , $i = 1, \dots, n-1$. More precisely, due to Relation (4.2) below, $F(t, T_i, T_{i+1})$ is a geometric Brownian motion under \mathbb{P}_{i+1} , $i = 0, \dots, n-1$, making it possible to apply the Black-Scholes pricing formula. In case $d \geq n$ the system (4.1) can be rewritten using a $n-1$ -dimensional Brownian motion, hence without loss of generality one can take $d \leq n-1$.

In order to derive (4.1) we start from the definition

$$F(t, T_i, T_{i+1}) := \frac{1}{\delta_i} \left(\frac{P(t, T_i)}{P(t, T_{i+1})} - 1 \right),$$

which implies

$$dF(t, T_i, T_{i+1}) = \frac{1}{\delta_i} d \left(\frac{P(t, T_i)}{P(t, T_{i+1})} \right)$$

$$\begin{aligned}
&= \frac{1}{\delta_i} \frac{P(t, T_i)}{P(t, T_{i+1})} (\zeta_i(t) - \zeta_{i+1}(t))^\dagger \cdot (dW_t - \zeta_{i+1}(t)dt) \\
&= \frac{1}{\delta_i} (1 + \delta_i F(t, T_i, T_{i+1})) (\zeta_i(t) - \zeta_{i+1}(t)) \cdot (dW_t - \zeta_{i+1}(t)dt) \\
&= \frac{1}{\delta_i} (1 + \delta_i F(t, T_i, T_{i+1})) (\zeta_i(t) - \zeta_{i+1}(t)) \cdot dW_t^{i+1}.
\end{aligned}$$

Assuming the existence of a deterministic \mathbb{R}^d -valued function $\gamma_i(t)$ such that

$$(\zeta_i(t) - \zeta_{i+1}(t))(1 + \delta_i F(t, T_i, T_{i+1})) = \delta_i \gamma_i(t) F(t, T_i, T_{i+1}), \quad i = 0, \dots, n-1, \quad (4.2)$$

we get

$$\begin{aligned}
\frac{dF(t, T_i, T_{i+1})}{F(t, T_i, T_{i+1})} &= \gamma_i^\dagger(t) \cdot dW_t^{i+1} \\
&= \gamma_i^\dagger(t) \cdot (dW_t^k + (\zeta_k(t) - \zeta_{i+1}(t))dt) \\
&= \gamma_i^\dagger(t) \cdot \left(dW_t^k - \sum_{j=i+1}^{k-1} (\zeta_j(t) - \zeta_{j+1}(t))dt \right) \\
&= \gamma_i^\dagger(t) \cdot \left(dW_t^k - \sum_{j=i+1}^{k-1} \frac{\delta_j \gamma_j(t) F(t, T_j, T_{j+1})}{1 + \delta_j F(t, T_j, T_{j+1})} dt \right),
\end{aligned}$$

$0 \leq t \leq T_i$, $1 \leq i < k \leq n$, and similarly for $1 \leq k \leq i < n$:

$$\begin{aligned}
\frac{dF(t, T_i, T_{i+1})}{F(t, T_i, T_{i+1})} &= \gamma_i^\dagger(t) \cdot \left(dW_t^k + \sum_{j=k}^i (\zeta_j(t) - \zeta_{j+1}(t))dt \right) \\
&= \gamma_i^\dagger(t) \cdot \left(dW_t^k + \sum_{j=k}^i \frac{\delta_j \gamma_j(t) F(t, T_j, T_{j+1})}{1 + \delta_j F(t, T_j, T_{j+1})} dt \right).
\end{aligned}$$

In particular, for $k = n$ we have

$$\frac{dF(t, T_i, T_{i+1})}{F(t, T_i, T_{i+1})} = \gamma_i^\dagger(t) \cdot \left(dW_t^n - \sum_{j=i+1}^{n-1} \frac{\delta_j \gamma_j(t) F(t, T_j, T_{j+1})}{1 + \delta_j F(t, T_j, T_{j+1})} dt \right),$$

$0 \leq t \leq T_i$, which is a martingale under \mathbb{P}_{i+1} , $i = 1, \dots, n-1$.

Remark - Alternative derivation

It is also possible to derive the BGM stochastic differential equation (4.1) by replacing condition (4.2) by the assumption that $F(t, T_i, T_{i+1})$ is a geometric Brownian motion under \mathbb{P}_{i+1} , i.e.

$$\frac{dF(t, T_i, T_{i+1})}{F(t, T_i, T_{i+1})} = \gamma_i^\dagger(t) \cdot dW_t^{i+1}$$

for some deterministic \mathbb{R}^d -valued function $\gamma_i(t)$, $i = 1, \dots, n-1$. From Proposition 3.3 we have

$$\Psi_i(t) := \mathbb{E}_{i+1} \left[\frac{d\mathbb{P}_i}{d\mathbb{P}_{i+1}} \middle| \mathcal{F}_t \right] = \frac{P(0, T_{i+1})}{P(t, T_{i+1})} \frac{P(t, T_i)}{P(0, T_i)} = \frac{P(0, T_{i+1})}{P(0, T_i)} (1 + \delta_i F(t, T_i, T_{i+1})),$$

hence by Itô's calculus,

$$d\Psi_i(t) = \delta_i \frac{P(0, T_{i+1})}{P(0, T_i)} F(t, T_i, T_{i+1}) \gamma_i^\dagger(t) \cdot dW_t^{i+1} = \delta_i \Psi_i(t) \frac{F(t, T_i, T_{i+1})}{1 + \delta_i F(t, T_i, T_{i+1})} \gamma_i^\dagger(t) \cdot dW_t^{i+1},$$

and by the Girsanov theorem,

$$dF(t, T_i, T_{i+1}) - \frac{1}{\Psi_i(t)} d\langle \Psi_i(t), F(t, T_i, T_{i+1}) \rangle = dF(t, T_i, T_{i+1}) - \delta_i \frac{F^2(t, T_i, T_{i+1}) \gamma_i^\dagger(t) \cdot \gamma_i(t)}{1 + \delta_i F(t, T_i, T_{i+1})} dt$$

is a continuous martingale under \mathbb{P}_i with quadratic variation $F^2(t, T_i, T_{i+1}) \gamma_i(t)^\dagger \cdot \gamma_i(t) dt$, hence

$$\frac{dF(t, T_i, T_{i+1})}{F(t, T_i, T_{i+1})} = \gamma_i^\dagger(t) \cdot dW_t^{i+1} = \gamma_i^\dagger(t) \cdot dW_t^i + \frac{\delta_i F(t, T_i, T_{i+1}) \gamma_i^\dagger(t) \cdot \gamma_i(t)}{1 + \delta_i F(t, T_i, T_{i+1})} dt,$$

where W_t^i is a Brownian motion under \mathbb{P}_i , with the relation

$$dW_t^{i+1} = dW_t^i + \frac{\delta_i F(t, T_i, T_{i+1}) \gamma_i(t)}{1 + \delta_i F(t, T_i, T_{i+1})} dt,$$

which eventually recovers (4.1), and also implies (4.2) in view of (3.2).

5 Pricing of caps and swaptions

The caplet payoff

$$\delta_i (L(T_i, T_{i+1}) - \kappa)^+$$

is priced as time $t \in [0, T_i]$ as

$$\begin{aligned} \delta_i \mathbb{E} \left[e^{-\int_t^{T_{i+1}} r_s ds} (L(T_i, T_{i+1}) - \kappa)^+ \middle| \mathcal{F}_t \right] &= \delta_i P(t, T_{i+1}) \mathbb{E}_{i+1} [(L(T_i, T_{i+1}) - \kappa)^+ \mid \mathcal{F}_t] \\ &= \delta_i P(t, T_{i+1}) \text{Bl}(\kappa, F(t, T_i, T_{i+1}), \sigma_i(t), T_i - t), \end{aligned}$$

from (3.1) and the Black-Scholes formula

$$\text{Bl}(\kappa, F(t, T_i, T_{i+1}), \sigma_i(t), T_i - t) = F(t, T_i, T_{i+1}) \Phi(d_1) - \kappa \Phi(d_2),$$

with

$$\Phi(x) = \frac{1}{\sqrt{2\pi}} \int_{-\infty}^x e^{-y^2/2} dy, \quad x \in \mathbb{R},$$

where

$$d_1 = \frac{\log(F(t, T_i, T_{i+1})/\kappa) + \sigma_i^2(t)(T_i - t)/2}{\sigma_i(t)\sqrt{T_i - t}}, \quad d_2 = d_1 - \sigma_i(t)\sqrt{T_i - t},$$

and

$$|\sigma_i(t)|^2 = \frac{1}{T_i - t} \int_t^{T_i} \gamma_i^\dagger(s) \cdot \gamma_i(s) ds. \quad (5.1)$$

This formula can be used to recover the caplet volatilities $\sigma_i^B(t)$ from market data as in the following table, where the time to maturity $T_i - t$ is in ordinate and the period $T_j - T_i$ is in abscissa, cf. Figure 5.1 below. This table and other data used in this paper has been communicated to the authors in 2005 by IXIS Corporate Investment Bank, Paris.

	Vol Cap At the Money	1M	3M	6M	12M	2Y	3Y	4Y	5Y	7Y	10Y
2D		9,25	9	8,85	18,6	18	16,8	15,7	14,7	13	11,3
1M		15,35	15,1	14,95	17,6	18,03	16,83	15,73	14,73	13,03	11,33
2M		15,75	15,5	15,35	18,1	18,41	17,11	16,01	15,01	13,26	11,56
3M		15,55	15,3	15,15	18,6	18,79	17,39	16,29	15,29	13,49	11,79
6M		17,55	17,3	17,15	18,7	18,28	16,98	15,88	14,98	13,48	11,98
9M		18,35	18,1	17,95	18,3	17,76	16,56	15,51	14,66	13,31	12,01
1Y		19,25	19	18,85	17,9	17,25	16,15	15,15	14,35	13,15	12,05
2Y		17,85	17,6	17,45	16,3	15,96	15,16	14,46	13,86	12,96	12,06
3Y		16,8	16,55	16,4	15,2	15,38	14,58	13,98	13,58	12,88	12,18
4Y		15,6	15,35	15,2	14,4	14,79	14,19	13,69	13,29	12,79	12,29
5Y		14,65	14,4	14,25	13,4	14,5	13,97	13,53	13,2	12,8	12,4
6Y		13,8	13,55	13,45	12,85	14,19	13,66	13,17	12,89	12,54	12,14
7Y		13,35	13,1	13	12,3	13,88	13,35	12,81	12,58	12,28	11,88
8Y		13,1	12,85	12,75	11,97	13,65	13,15	12,65	12,42	12,12	11,75
9Y		12,75	12,5	12,4	11,63	13,43	12,96	12,49	12,26	11,96	11,63
10Y		12,4	12,15	12,05	11,3	13,5	13,02	12,53	12,25	11,89	11,5
12Y		11,85	11,6	11,5	10,8	13,22	12,75	12,28	12,01	11,69	11,3
15Y		11,25	11	10,9	10,2	13	12,55	12,1	11,85	11,57	11,15
20Y		10,45	10,2	10,1	9,5	11,9	11,55	11,2	11,05	11,03	10,8
25Y		9,7	9,45	9,35	8,8	11,68	11,33	10,98	10,83	10,68	10,55
30Y		9,05	8,8	8,7	8,1	11,45	11,1	10,75	10,6	10,72	10,3

Figure 5.1: Caplet volatilities.

In Figure 5.1 we will actually only make use of the data of a single column giving volatilities for a period δ equal to the fixed tenor value. The pricing of caplets can be extended to caps of the form

$$\sum_{k=i}^{j-1} \delta_k (L(T_k, T_{k+1}) - \kappa)^+$$

since they can be decomposed into a sum of caplets and are priced at time $t \in [0, T_i]$ as

$$\sum_{k=i}^{j-1} \delta_k P(t, T_{k+1}) \text{Bl}(\kappa, F(t, T_k, T_{k+1}), \sigma_k(t), 0, T_k - t).$$

In the case of the swaption

$$\left(\sum_{k=i}^{j-1} \delta_k P(T_i, T_{k+1}) (F(T_i, T_k, T_{k+1}) - \kappa) \right)^+,$$

the positive part can not be taken out of the sum, and in general the price of the swaption is smaller than the value of the corresponding cap.

This swaption is priced at time $t \in [0, T_i]$ as

$$\begin{aligned} & \mathbb{E} \left[e^{-\int_t^{T_i} r_s ds} \left(\sum_{k=i}^{j-1} \delta_k P(T_i, T_{k+1}) (F(T_i, T_k, T_{k+1}) - \kappa) \right)^+ \middle| \mathcal{F}_t \right] \\ &= \mathbb{E} \left[e^{-\int_t^{T_i} r_s ds} \left(P(T_i, T_i) - P(T_i, T_j) - \kappa \sum_{k=i}^{j-1} \delta_k P(T_i, T_{k+1}) \right)^+ \middle| \mathcal{F}_t \right] \\ &= \mathbb{E} \left[e^{-\int_t^{T_i} r_s ds} \sum_{k=i}^{j-1} \delta_k P(T_i, T_{k+1}) (S(T_i, T_i, T_j) - \kappa)^+ \middle| \mathcal{F}_t \right] \\ &= P(t, T_i) \mathbb{E}_i \left[\sum_{k=i}^{j-1} \delta_j P(T_i, T_{k+1}) (S(T_i, T_i, T_j) - \kappa)^+ \middle| \mathcal{F}_t \right] \\ &= P(t, T_i) \mathbb{E}_i \left[P(T_i, T_i, T_j) (S(T_i, T_i, T_j) - \kappa)^+ \middle| \mathcal{F}_t \right] \\ &= P(t, T_i, T_j) \mathbb{E}_{i,j} \left[(S(T_i, T_i, T_j) - \kappa)^+ \middle| \mathcal{F}_t \right], \end{aligned} \tag{5.2}$$

where the martingale measure $\mathbb{P}_{i,j}$ is defined by

$$\frac{d\mathbb{P}_{i,j}|\mathcal{F}_t}{d\mathbb{P}|\mathcal{F}_t} = \frac{e^{-\int_t^{T_i} r_s ds} P(T_i, T_i, T_j)}{P(t, T_i, T_j)}, \quad t \in [0, T_i],$$

i.e.

$$\frac{d\mathbb{P}_{i,j}|\mathcal{F}_t}{d\mathbb{P}_{i|\mathcal{F}_t}} = \frac{P(t, T_i) P(T_i, T_i, T_j)}{P(t, T_i, T_j)}, \quad t \in [0, T_i],$$

$1 \leq i < j \leq n$.

Swaption prices can be computed using the dynamics of $F(t, T_k, T_{k+1})$ under \mathbb{P}_i , $1 \leq i \leq k < j \leq n$, but the market practice is to use approximation formulas. When $j = i + 1$ we have $\mathbb{P}_{i,i+1} = \mathbb{P}_i$, the swaption price equals

$$P(t, T_i) \mathbb{E}_i \left[(L(T_i, T_{i+1}) - \kappa)^+ \middle| \mathcal{F}_t \right]$$

and is approximated by

$$P(t, T_i) \text{Bl}(\kappa, F(t, T_i, T_{i+1}), \sigma_i(t), 0, T_i - t).$$

The swaption approximation formula extends to general indices $1 \leq i < j \leq n$ as

$$P(t, T_i, T_j) \text{Bl}(\kappa, S(t, T_i, T_j), \sigma_{i,j}(t), 0, T_i - t), \quad (5.3)$$

where

$$|\sigma_{i,j}(t)|^2 = \sum_{l,l'=i}^{j-1} \frac{v_l^{i,j}(t)v_{l'}^{i,j}(t)F(t, T_l, T_{l+1})F(t, T_{l'}, T_{l'+1})}{(T_i - t)|S(t, T_i, T_j)|^2} \int_t^{T_i} \gamma_l^\dagger(s) \cdot \gamma_{l'}(s) ds, \quad (5.4)$$

$t \in [0, T_i]$, and

$$v_l^{i,j}(t) = \frac{\delta_l P(t, T_{l+1})}{P(t, T_i, T_j)}.$$

This approximation amounts to saying that $S(t, T_i, T_j)$, $t \in [0, T_i]$, is an exponential martingale with variance coefficient $\sigma_{i,j}(t)$ under $\mathbb{P}_{i,j}$, and (5.3) turns out to be quite accurate when compared to Monte Carlo evaluations of (5.2), cf. [8], §1.3.3.

Vol Swaption At The Money											
	1Y	2Y	3Y	4Y	5Y	6Y	7Y	8Y	9Y	10Y	25Y
2D	18.6	18	16.8	15.7	14.7	13.8	13	12.3	11.8	11.3	9.3
1M	17.6	18	16.8	15.7	14.7	13.8	13	12.3	11.8	11.3	9.3
2M	18.1	18.35	17.05	15.95	14.95	14	13.2	12.55	12	11.5	9.45
3M	18.6	18.7	17.3	16.2	15.2	14.2	13.4	12.8	12.2	11.7	9.6
6M	18.7	18.1	16.8	15.7	14.8	13.9	13.3	12.7	12.2	11.8	9.7
9M	18.3	17.5	16.3	15.25	14.4	13.6	13.05	12.55	12.1	11.75	9.7
1Y	17.9	16.9	15.8	14.8	14	13.3	12.8	12.4	12	11.7	9.7
2Y	16.3	15.2	14.4	13.7	13.1	12.6	12.2	11.9	11.6	11.3	9.3
3Y	15.2	14.2	13.4	12.8	12.4	12	11.7	11.5	11.2	11	9.2
4Y	14.4	13.2	12.6	12.1	11.7	11.5	11.2	11	10.8	10.7	8.8
5Y	13.4	12.4	11.9	11.5	11.2	11	10.8	10.7	10.5	10.4	8.6
6Y	12.85	11.95	11.45	11	10.75	10.55	10.4	10.25	10.1	10	8.3
7Y	12.3	11.5	11	10.5	10.3	10.1	10	9.8	9.7	9.6	8
8Y	11.97	11.13	10.67	10.2	10	9.8	9.7	9.53	9.43	9.33	7.83
9Y	11.63	10.77	10.33	9.9	9.7	9.5	9.4	9.27	9.17	9.07	7.67
10Y	11.3	10.4	10	9.6	9.4	9.2	9.1	9	8.9	8.8	7.5
12Y	10.8	10.04	9.58	9.28	9.02	8.92	8.76	8.66	8.56	8.46	7.38
15Y	10.2	9.5	9.1	8.8	8.6	8.5	8.4	8.3	8.2	8.1	7.2
20Y	9.5	8.8	8.5	8.2	8	8	8	8	7.9	7.9	6.9
25Y	8.8	8.1	7.9	7.6	7.4	7.5	7.6	7.7	7.6	7.7	6.6
30Y	8.1	7.4	7.3	7	6.8	7	7.2	7.4	7.3	7.5	6.3

Figure 5.2: Swaption volatilities.

Figure 5.2 above shows an example of market data expressed in terms of swaption volatilities $\sigma_{i,j}^B(t)$ by inversion of the swaption approximation formula (5.3). Here, the time to maturity $T_i - t$ is in ordinate and the period $T_j - T_i$ is in abscissa. This type of data can be also expressed in the form of a graph (Figure 5.3) where the index i refers to the time to maturity $T_i - t$ and the index j refers to the period $T_j - T_i$:

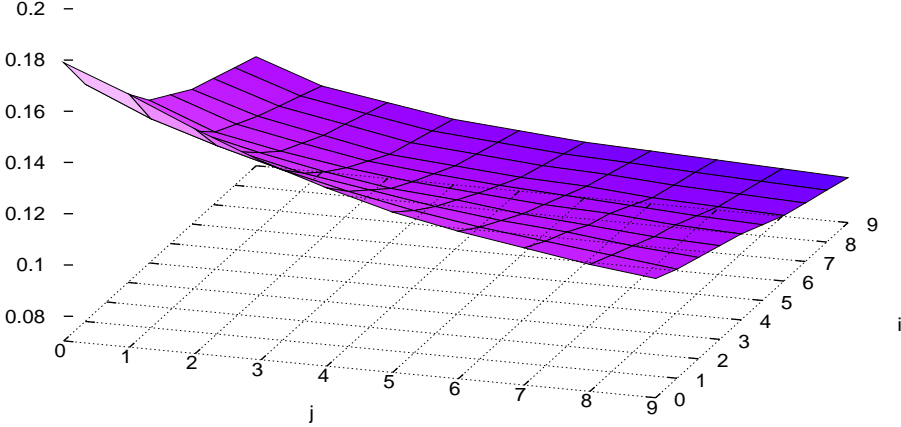


Figure 5.3: Market swaption volatilities.

Note that the swaption volatilities can be estimated in a different way, using the so-called Market Swaption Formula (MSF)

$$|\sigma_{i,j}^{MSF}(t)|^2 = \sum_{l,l'=i}^{j-1} \frac{v_l^{i,j}(t)v_{l'}^{i,j}(t)F(t, T_l, T_{l+1})F(t, T_{l'}, T_{l'+1})}{|S(t, T_i, T_j)|^2} \sigma_l^B(t)\sigma_{l'}^B(t) \text{Cor}_t(F(T_i, T_l, T_{l+1}), F(T_i, T_{l'}, T_{l'+1})), \quad (5.5)$$

$1 \leq i < j \leq n$, where $\sigma_i^B(t)$ are the Black caplet volatilities and

$$\text{Cov}_t(F, G) = \mathbb{E}[FG \mid \mathcal{F}_t] - \mathbb{E}[F \mid \mathcal{F}_t]\mathbb{E}[G \mid \mathcal{F}_t].$$

This formula can be used to reduce the numerical instabilities observed in the calibration procedure, see the next section.

6 LIBOR calibration

The goal of calibration is to estimate the volatility functions

$$\gamma_i(t) \in \mathbb{R}^d, \quad 1 \leq i \leq n,$$

appearing in the BGM model from the data of caps and swaptions prices observed on the market. This involves several computational and stability issues. Let

$$g_i^2(t) = \gamma_i^\dagger(t) \cdot \gamma_i(t), \quad i = 1, \dots, n,$$

and

$$\begin{aligned} \rho_{i,j}(t) &= \frac{\gamma_i^\dagger(t) \cdot \gamma_j(t)}{\left(\gamma_i^\dagger(t) \cdot \gamma_i(t)\right)^{1/2} \left(\gamma_j^\dagger(t) \cdot \gamma_j(t)\right)^{1/2}} \\ &= \frac{\gamma_i^\dagger(t) \cdot \gamma_j(t)}{g_i(t)g_j(t)}, \quad i, j = 1, \dots, n. \end{aligned}$$

We use the Rebonato [6] parameterization:

$$g_i(t) = c_i g(T_i - t), \quad i = 1, \dots, n,$$

where

$$g(t) = g_\infty + (1 + at - g_\infty)e^{-bt}, \quad a, b, g_\infty > 0,$$

and the correlation coefficients ρ_{ij} are time independent and parameterized by η_1 , η_2 and ρ_∞ , as in Relation (13) of [7], i.e.

$$\begin{aligned} \rho_{ij} &= \exp\left(-\frac{|i-j|}{n-1}\left(\eta_1 \frac{i^2 + j^2 + ij - 3(n-1)(i+j) + 2n^2 - n - 4}{(n-2)(n-3)}\right.\right. \\ &\quad \left.\left.- \eta_2 \frac{i^2 + j^2 + ij - (n+3)(i+j) + 3n + 2}{(n-2)(n-3)} - \log \rho_\infty\right)\right), \quad i, j = 1, \dots, n, \end{aligned}$$

see also § 2.3.4 of [8]. After equating

$$|\sigma_i^B(t)|^2 = \frac{1}{T_i - t} \int_t^{T_i} \gamma_i^\dagger(s) \cdot \gamma_i(s) ds = \frac{1}{T_i - t} \int_t^{T_i} g_i^2(s) ds$$

as in (5.1), one obtains from (5.4) the expression

$$\begin{aligned} &\sigma_{i,j}(t, b, g_\infty, \eta_1, \eta_2, \rho_\infty) \\ &= \sqrt{\sum_{l,l'=i}^{j-1} \frac{v_l^{i,j}(t)v_{l'}^{i,j}(t)F(t, T_l, T_{l+1})F(t, T_{l'}, T_{l'+1})}{(T_i - t)|S(t, T_i, T_j)|^2} \int_t^{T_i} g_l(s)g_{l'}(s)\rho_{l,l'}(s)ds} \\ &= \sqrt{\sum_{l,l'=i}^{j-1} \frac{\rho_{l,l'}\alpha_{l,l'}(t)\sigma_l^B(t)\sigma_{l'}^B(t)v_l^{i,j}(t)v_{l'}^{i,j}(t)F(t, T_l, T_{l+1})F(t, T_{l'}, T_{l'+1})}{(T_i - t)|S(t, T_i, T_j)|^2}} \end{aligned}$$

of $\sigma_{i,j}(t)$ as a function of $b, g_\infty, \eta_1, \eta_2, \rho_\infty$, where

$$\begin{aligned}\alpha_{l,l'}(t) &= \frac{\sqrt{T_l - t} \sqrt{T_{l'} - t} \int_t^{T_l} g_l(s) g_{l'}(s) ds}{\sqrt{\int_t^{T_l} g_l^2(s) ds} \sqrt{\int_t^{T_{l'}} g_{l'}^2(s) ds}} \\ &= \frac{\sqrt{T_l - t} \sqrt{T_{l'} - t} \int_0^{T_l - t} (g_\infty + (1 - g_\infty)e^{-bs})^2 ds}{\sqrt{\int_0^{T_l - t} (g_\infty + (1 - g_\infty)e^{-bs})^2 ds} \sqrt{\int_t^{T_{l'} - t} (g_\infty + (1 - g_\infty)e^{-bs})^2 ds}},\end{aligned}$$

and a is set equal to 0.

Following again [7] we minimize the mean square distance

$$\text{RMS}(b, g_\infty, \eta_1, \eta_2, \rho_\infty) := \sqrt{\frac{2}{(n-1)(n-2)} \sum_{i=1}^k \sum_{j=i+1}^n \left(\frac{\sigma_{i,j}^B(t) - \sigma_{i,j}(t)}{\sigma_{i,j}^B(t)} \right)^2},$$

where n is the number of tenor dates (in multiples of one year) and k is the maximum number of swaption maturities used in the calibration, with non-available data treated as zero in the sum. The data of discount factors and swap rates are interpolated with a fixed tenor $\delta = \text{half year}$.

Minimization is done using the Broyden-Fletcher-Goldfarb-Shanno (BFGS) gradient descent method for nonconvex objective functions. The volatilities computed in this way are given in Figure 6.1, where the index i refers to $T_i - t$ and j refers to $T_j - T_i$:

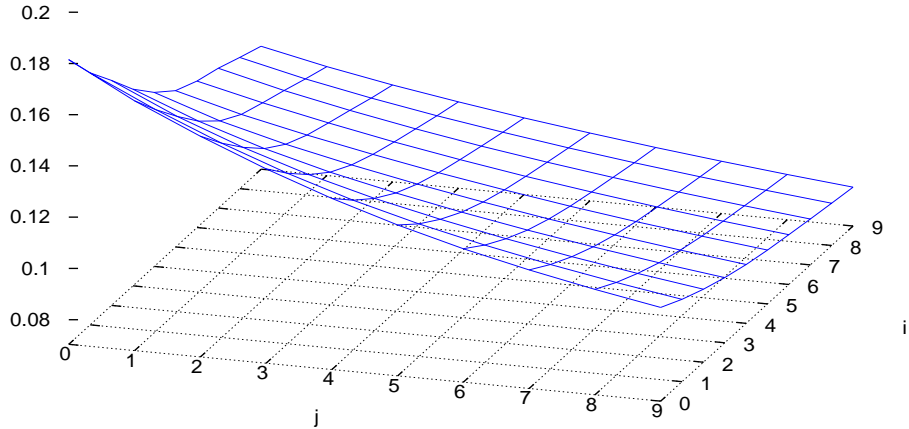


Figure 6.1: Computed swaption volatilities.

The next graph (Figure 6.2) allows us to compare the estimated and computed volatilities:

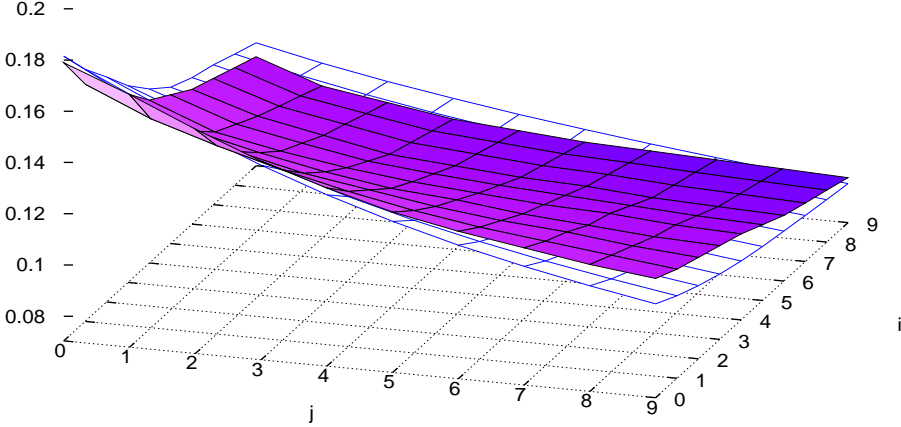


Figure 6.2: Comparison graphs.

We also applied the more stable MSF calibration algorithm designed in [7] from the market swaption formula. For this the correlations $\text{Cor}_t(F(T_i, T_l, T_{l+1}), F(T_i, T_{l'}, T_{l'+1}))$ appearing in (5.5) are estimated by

$$\text{Cor}_t(F(T_i, T_l, T_{l+1}), F(T_i, T_{l'}, T_{l'+1})) \sim \frac{\int_t^{T_i} g(T_l - s)g(T_{l'} - s)ds}{\sqrt{\int_t^{T_i} g^2(T_l - s)ds} \sqrt{\int_t^{T_i} g^2(T_{l'} - s)ds}} \rho_{l,l'}(t),$$

which yields an expression of $\sigma_{i,j}^{\text{MSF}}(t)$ as a function

$$\sigma_{i,j}^{\text{MSF}}(t, b, g_\infty, \eta_1, \eta_2, \rho_\infty)$$

of $b, g_\infty, \eta_1, \eta_2, \rho_\infty$, cf. [7]. The mean square distance associated to the MSF formula is then defined as

$$\text{RMS}^{\text{MSF}}(b, g_\infty, \eta_1, \eta_2, \rho_\infty) = \sqrt{\frac{2}{(n-1)(n-2)} \sum_{i=1}^k \sum_{j=i+1}^n \left(\frac{\sigma_{i,j}^B(t) - \sigma_{i,j}^{\text{MSF}}(t)}{\sigma_{i,j}^B(t)} \right)^2},$$

and we minimize the objective function

$$\text{RMS}^{\text{MSF}}(b, g_\infty, \eta_1, \eta_2, \rho_\infty) \max(\text{RMS}(b, g_\infty, \eta_1, \eta_2, \rho_\infty), \text{RMS}^{\text{MSF}}(b, g_\infty, \eta_1, \eta_2, \rho_\infty)).$$

A sample of joint numerical estimation of the five parameters $(b, g_\infty, \eta_1, \eta_2, \rho_\infty)$ is given in the next table (Figure 6.3), where the maximum number k of swaption maturities

used in each calibration is denoted by UpToMat. The total number of swaptions used is bounded by $nk - k(k + 1)/2$.

UpToMat	#swaptions	b	g_∞	η_1	η_2	ρ_∞	RMS
1	10	5.03	0.85	1.95	0.15	0.010	0.008
2	20	5.03	0.71	2.00	0.13	0.11	0.010
3	30	5.04	0.73	1.86	0.13	0.08	0.010
4	40	5.03	0.72	2.00	0.09	0.09	0.010
5	50	5.04	0.70	1.27	0.03	0.06	0.011
6	60	5.03	0.65	0.56	0.00	0.03	0.011
7	70	5.02	0.60	0.15	0.00	0.01	0.012
8	80	5.02	0.60	0.01	0.00	0.09	0.012
9	90	5.02	0.72	0.70	0.00	0.01	0.013
10	100	5.04	0.63	0.01	0.00	0.01	0.012
12	110	5.03	0.65	0.01	0.00	0.004	0.012
15	120	5.03	1.00	0.701	0.00	0.002	0.014

Figure 6.3: Numerical results.

Our program allows the user to choose the parameters to be estimated, and calibrating less parameters at a time while fixing the values of the others yields more stable results. The program also makes use of available smile data given by shifts of volatilities according to the following tables, for swaptions in Figure 6.4:

Vol Cap CMS Smile	Shift compared to ATM												
	-5	-2	-1	-0.5	-0.25	0	0.25	0.5	1	2	5	10	20
1Y	17.65	3.75	1.25	0.25	-0.25	-0.35	-0.3	-0.1	0.45	1.55	5.65	11.4	16.65
5Y	14.4	1.9	-0.5	-1.6	-1.9	-2.1	-2.1	-2	-1.95	-1.2	1.8	5.9	10.1
10Y	9.6	0.4	-1.7	-2.6	-2.75	-2.95	-2.9	-2.85	-2.8	-2	0.35	3.55	7.4
15Y	8.1	-0.3	-1.9	-2.6	-2.7	-2.85	-2.85	-2.8	-2.7	-2.05	0.15	3.1	6.5
20Y	6.63	-0.78	-1.88	-2.38	-2.48	-2.58	-2.58	-2.53	-2.48	-2.13	0.03	2.73	5.73
30Y	5.05	-1.3	-2.05	-2.15	-2.25	-2.25	-2.25	-2.25	-2.25	-2.2	-0.25	2.15	4.8

10Y													
	-5	-2	-1	-0.5	-0.25	0	0.25	0.5	1	2	5	10	20
1Y	17.65	3.75	1.25	0.25	-0.25	-0.35	-0.3	-0.1	0.45	1.75	5.9	11.9	17.3
5Y	13.5	1.9	-0.7	-1.55	-1.9	-2	-2	-1.85	-1.55	-0.5	2.75	6.95	11.05
10Y	8.9	0.1	-1.6	-2.3	-2.35	-2.4	-2.4	-2.3	-1.95	-1	1.7	5.25	8.8
15Y	6.8	-0.85	-2.1	-2.4	-2.55	-2.65	-2.5	-2.45	-2.05	-1.2	1.4	4.6	7.75
20Y	5.4	-1.05	-2.1	-2.25	-2.3	-2.35	-2.3	-2.2	-1.8	-1.15	1.3	4.2	7
30Y	3.8	-1.55	-2.05	-2.05	-2.05	-2.05	-2	-1.9	-1.7	-1.05	1.1	3.6	6

Figure 6.4: Smile data for caps.

and for caps in Figure 6.5:

Vol Cap Libor Smile	1M	Shift compared to ATM											
	-5	-2	-1	-0.5	-0.25	0	0.25	0.5	1	2	5	10	20
1Y	20	6,5	2,75	1	0,5	0	0,05	0,1	0,15	0,5	3,5	7	10,5
5Y	17,75	4,7	1,75	0,6	0,15	0	0,05	0,05	0,1	0,4	3,2	7	10,5
10Y	15,5	3,75	0,9	0,3	0,05	0	0,03	0,05	0,05	0,25	2,3	5,5	8
30Y	9	1,75	0,25	0,15	0	0	0	0,05	0,1	1,5	4	6	

Vol Cap Libor Smile	3M	Shift compared to ATM											
	-5	-2	-1	-0.5	-0.25	0	0.25	0.5	1	2	5	10	20
1Y	20	6,5	2,75	1	0,5	0	0,05	0,1	0,15	0,5	3,5	7	10,5
5Y	17,75	4,7	1,75	0,6	0,15	0	0,05	0,05	0,1	0,4	3,2	7	10,5
10Y	15,5	3,75	0,9	0,3	0,05	0	0,03	0,05	0,05	0,25	2,3	5,5	8
30Y	9	1,75	0,25	0,15	0	0	0	0,05	0,1	1,5	4	6	

Figure 6.5: Smile data for swaptions.

References

- [1] A. Brace, D. Gatarek, and M. Musiela. The market model of interest rate dynamics. *Math. Finance*, 7(2):127–155, 1997.
- [2] D. Brigo and F. Mercurio. *Interest rate models—theory and practice*. Springer Finance. Springer-Verlag, Berlin, second edition, 2006.
- [3] R. A. Carmona and M. R. Tehranchi. *Interest rate models: an infinite dimensional stochastic analysis perspective*. Springer Finance. Springer-Verlag, Berlin, 2006.
- [4] F. Jamshidian. LIBOR and swap market models and measures. *Finance and Stochastics*, 1(4):293–330, 1997.
- [5] N. Privault. *An Elementary Introduction to Stochastic Interest Rate Modeling*, volume 12 of *Advanced Series on Statistical Science & Applied Probability*. World Scientific Publishing Co. Inc., River Edge, NJ, 2008. ISBN 978-981-283-273-3.
- [6] R. Rebonato. *Interest-Rate Option Models*. John Wiley & Sons, 1996.
- [7] J. Schoenmakers. Calibration of LIBOR models to caps and swaptions: a way around intrinsic instabilities via parsimonious structures and a collateral market criterion. WIAS Preprint No 740, Berlin, 2002.
- [8] J. Schoenmakers. *Robust LIBOR modelling and pricing of derivative products*. Chapman & Hall/CRC Financial Mathematics Series. Chapman & Hall/CRC, Boca Raton, FL, 2005.